

Modelling of Thermal Conductivity for High Burnup UO₂ Fuel Retaining Rim Region

Byung-Ho Lee, Yang-Hyun Koo, and Dong-Seong Sohn

Korea Atomic Energy Research Institute
150 Dukjin-dong, Yusong-gu, Taejon 305-353, Korea

(Received August 12, 1995)

Abstract

A thermal conductivity correlation has been proposed which can be applied to high burnup fuel by considering both of thermal conductivity with burnup across fuel pellet and additional degradation at pellet rim due to very high porosity. In addition, a correlation has been developed that can estimate the porosity of rim region as a function of rim burnup under the assumptions that all the produced fission gases are retained in the rim porosity and threshold pellet average burnup required for the formation of rim region is 40 MWD/kgU. Rim width is correlated to rim burnup using measured data.

For the RISO experimental data obtained at pellet average burnup of 43.5 MWD/kgU for three linear heat generation rates of 30, 35 and 40 kW/m, radial temperature distributions were calculated using the present correlation and compared with the measured ones. This comparison shows that the present correlation gives the best agreement with the measured data when it is combined with the HALDEN's correlation for thermal conductivity considering its degradation with burnup. Another comparison with the HALDEN's measured fuel centerline temperature as a function of burnup at 25 kW/m up to about 44 MWD/kgU also suggests that the present correlation yields the best agreement when it is combined with the HALDEN's thermal conductivity.

1. Introduction

Fuel temperature controls almost all physical processes related to in-reactor fuel behavior. Since more fission gases are available for release and swelling in high burnup fuel, temperature is one of the most important operating parameters in high burnup fuel. In addition, the amount of stored energy in pellet rim during reactivity initiated accident (RIA) condition, which has recently been regarded as a great concern with respect to fuel failure, is also influenced by the fuel temperature. A good prediction of temperature is therefore an essential requirement for the performance analysis of high burnup fuel.

Radial power density distribution in fuel rods is nonuniform and is a function of burnup, initial enrichment and fuel rod geometry. At the beginning of irradiation, i.e., at low burnup, the concentration of fissile material is constant, which means that the radial power has a relatively small variation across pellet radius. At high burnup, however, there is a wide variation in this concentration with a marked increase in the ²³⁹Pu concentration near the pellet surface [1]. Furthermore, thermal conductivity is degraded with burnup because fission-gas bubble formation, pores, cracks, fission products buildup (dissolved and precipitated), and possible change in the oxygen to uranium ratio (O/U), which increase with irradiation, re-

duce the heat flow through phonon-defect and phonon-phonon scattering processes by introducing defects proportional to burnup.

In addition, the vicinity of pellet edge, i.e., rim region plays a significant role in heat flow as thermal barrier [2] which is characterized by loss of optically definable grain structure, an increase in small intragranular porosity, and a depletion of matrix xenon as measured by electron probe microanalysis (EPMA). Consequently rim effect has to be considered at high burnup fuel because high porous rim region induces the additional decrease in thermal conductivity after threshold pellet average burnup of about 40 MWD/kgU.

In the present study, a thermal conductivity correlation considering both the thermal conductivity degradation with burnup and additional decrease in the rim region due to high porosity is developed to predict an accurate temperature distribution.

2. Analysis Method

2.1. Rim Burnup and Rim Width

The rim which acts as thermal barrier develops in the periphery of pellet where local burnup is enhanced by plutonium production and fissioning in a low temperature. The enhanced local burnup results from the strong resonance absorption of neutrons in ^{238}U leading to a surface enrichment in ^{239}Np and therefore also in ^{239}Pu and thus in fission rate and local burnup [3]. This region, which could be formed in high-burnup fuel, can be characterized by very high porosity, marked decrease in UO_2 grain size, and depletion of xenon from UO_2 matrix as measured by EPMA.

To characterize the rim region, rim burnups (pellet-edge burnups) are correlated from measured experimental results [4,5]. Fig. 1 shows the rim burnup as a function of pellet average burnup. The rim burnup can be obtained from pellet-averaged burnup by least square method :

$$BU_{\text{Rim}} = 1.43 \cdot BU_{\text{avg}} \quad (1)$$

where BU_{Rim} is rim burnup and BU_{avg} average burnup of a pellet. A rim-to-average burnup ratio of 1.43 is consistent with the value measured in RISO project, as well as with transport theory [6]. In this analysis the threshold pellet average burnup for the formation of rim region is assumed to be 40 MWD/kgU.

Another characteristic of rim region, rim width is estimated by using the measured data [7,8]. EPMA data are chosen for the analysis due to larger fluctuation of optical microscopy (OM) data even though the width could be determined by both OM and EPMA. Fig. 2 shows the fitted rim width as a function of rim burnup with experimental data. The least square method using linear relationship yields the following formula between rim width and rim burnup :

$$R_{\text{Rim}} = -305.8 + 5.24 \cdot BU_{\text{Rim}} \quad (2)$$

where R_{Rim} is the rim width in μm and BU_{Rim} rim burnup calculated from Eq. (1). Barner's relation [7] by using a parabolic dependence is also shown in Fig. 2. The relation was expressed by

$$R_{\text{Rim}}^2 = -21014 + 391.4 \cdot BU_{\text{Rim}} \quad (3)$$

Compared with Barner's relation, linear relationship

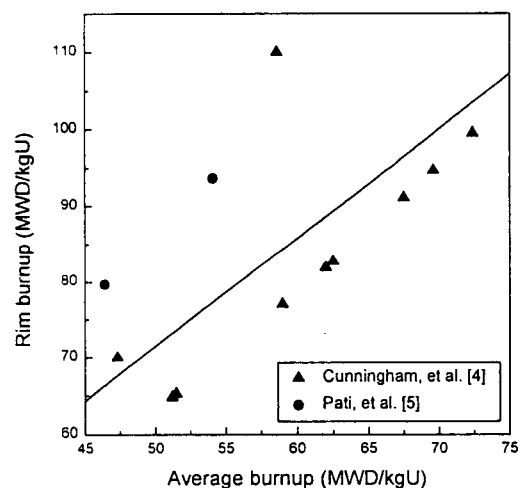


Fig. 1. Variation of Rim Burnup as a Function of Pellet Average Burnup

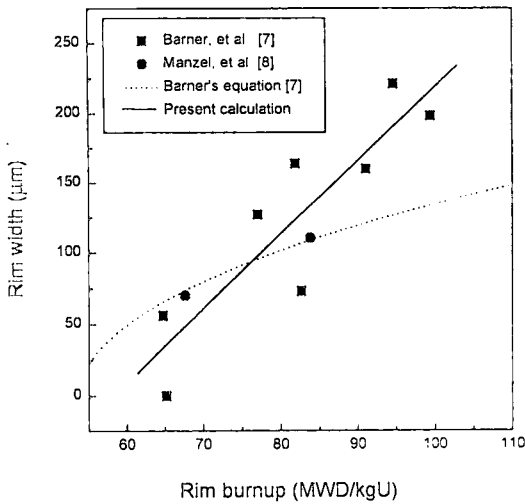


Fig. 2. Variation of Rim Width as a Function of Pellet edge Burnup

of Eq. (2) can be considered more reasonable because the rim width could be larger than 200 μm at very high burnup.

2.2. Porosity in the Rim Region

In LWR fuel the pellet rim starts to become very porous at average burnup of 40~45 MWD/kgU. Generally, the level of porosity ranges from 10 to 30 vol %.

For the simplified analysis of porosity in the rim region it is assumed that 3 stable fission gas atoms are generated from every 100 nuclear fission and produced fission gases consist of about 90% xenon and 10% krypton. Although it was reported that the xenon in the rim region is released to free volume of fuel, X-ray fluorescence analysis (XRF) and X-ray mapping results indicate that nearly all of the xenon produced in the rim region do not escape to free volume but are retained in the matrix. This also implies that the lost matrix xenon could be retained in the porosity of the rim region [4]. Furthermore, as yet no microcracks have been detected in the structure and there is no evidence to suggest that the pores are

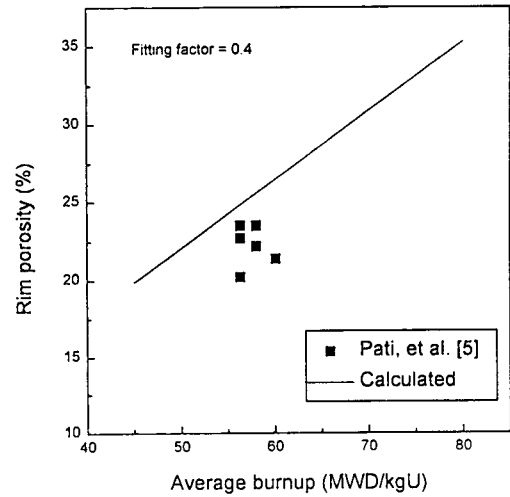


Fig. 3. Comparison Between Calculated and Measured Porosity at the Rim Region.

interconnected. Therefore it is a reasonable assumption that the produced xenon gas is contained in the newly formed pores [9].

The mass of heavy metal in the rim region in a pellet, M_{Rim} is given by

$$M_{Rim} = V_{Rim} \cdot \rho \quad (4)$$

where the volume of rim region, V_{Rim} is obtained from the rim width and ρ is the density of a pellet. Energy produced in the rim region, E_{Rim} is given by

$$E_{Rim} = M_{Rim} \cdot BU_{Rim} \quad (5)$$

Using the assumption that energy released per fission is 200 MeV, the generated fission gas volume is calculated to be 31.79 cm³/MWD at STP [Standard Temperature (0°C) and Pressure (1 atm)]. Then the total fission gas produced at the pellet rim is expressed by

$$V_0 = 31.79 \cdot E_{Rim} \quad (6)$$

where V_0 is produced total fission gas volume at STP. Then the total fission gas volume under reactor operating condition is approximated by simple ideal gas law

$$V_{op} = \phi \cdot \left(\frac{P \cdot V}{T} \right)_o \cdot \left(\frac{T}{P} \right)_{op} \quad (7)$$

where ϕ is a fitting factor to fit the measured porosity in the rim region and subscripts o and op represent the properties at STP and operating condition, respectively. Using Eq. (7), the fitting factor was obtained. When the porosity of the rim region is calculated using Eq. (7) under typical PWR operating condition, porosity in the rim region is correlated with rim burnup. The fitting factor of 0.4 was obtained as shown in Fig. 3 which covers the experimental data [5].

2.3. Thermal Conductivity Across the Fuel Pellet and in the Rim Region

Thermal conductivity for fuel pellet which considers the degradation effect of burnup is generally described as follows :

$$k = \frac{1}{(A + \beta \cdot BU + C \cdot T)} + D \cdot \text{EXP}(-E \cdot T) \quad (8)$$

where $\beta \cdot BU$ is the term to consider the thermal conductivity degradation with burnup. A hyperbolic term results from the lattice contribution through phonon-defect and phonon-phonon scattering processes and an exponential term from the electronic conduction which becomes dominant for high temperature larger than 1900 K. The cause of the degradation phenomenon is a result of the introduction by irradiation of defects to the previously almost perfect UO_2 lattice. Furthermore, thermal conductivity steeply decreases across the rim with burnup because of the porous microstructure and higher local fissioning. Consequently the thermal conductivity of irradiated UO_2 fuel is dependent on porosity, stoichiometry and burnup as well as temperature [8]. Constants for three thermal conductivities of MATPRO [11], SIMFUEL [8], and HALDEN [12] chosen for the present analysis are given in Table 1.

The decrease in thermal conductivity in the rim re-

Table 1. Constants for Thermal Conductivity at 95% Theoretical Density UO_2

	MATPRO [11]	SIMFUEL [10]
A	0.04670	0.053
b	0.0	0.0016
C	$2.294 \cdot 10^{-4}$	$(2.2 - 0.0005 \cdot BU) \cdot 10^{-4}$
D	$1.0 \cdot 10^{-2}$	0.0
E	$1.767 \cdot 10^{-3}$	0.0

Note : Constants for HALDEN's thermal conductivity could not be given here because it is a proprietary information of the NFIR program.

gion results in temperature jump at the pellet-edge. This temperature jump causes increase in the centerline temperature of a pellet which can lead to the violation of the design criterion for fuel centerline temperature.

In the rim region, the thermal conductivity degradation is obtained under the assumption that the rim region consists of pores and fully dense material. The dependence of thermal conductivity on porosity is given as follows [13] :

$$k_{Rim} = k_0 \cdot \left\{ 1 - a \cdot P_{Rim}^{\frac{2}{3}} \cdot \left[1 - \frac{1}{1 + \frac{1}{a} \cdot P_{Rim}^{\frac{1}{3}} \cdot (\nu - 1)} \right] \right\} \quad (9)$$

where

k_{Rim} = thermal conductivity of the porous rim (W/m · K)

k_0 = thermal conductivity of the fully dense material (W/m · K)

$$= k/[1 - (2.58 - 0.58 \times 10^{-3}T)P] [17]$$

$\nu = \frac{k_0}{k_p}$ (k_p is the thermal conductivity of the pore)

P = porosity (volume fraction of the porous phase)

a = anisotropy factor ($a=1$ means isotropic pore distribution)

The obtained k_0 is shown in Fig. 4 as dash line. It is noted that thermal conductivity of MATPRO is inde-

pendent of burnup, while the others decrease with burnup.

For the analysis of the thermal conductivity of pores in the rim region, it is assumed that all the xenon gas produced in the rim region are retained in the porosity. Then the thermal conductivity of porosity in Eq. (9) can be replaced by thermal conductivity of xenon [13] expressed by

$$k_{Xe} = 0.72 \times 10^{-4} \cdot T^{0.79} \quad (10)$$

Under the assumption that all the pores are isotropically distributed, i.e., α is equal to 1, thermal conductivity of the rim is shown in Fig. 4 as solid line for the temperature of 500°C. The thermal conductivity decreases abruptly around the pellet average burnup of 40 MWD/kgU. Fig. 4 shows that the thermal conductivity calculated by the HALDEN correlation is lowest among three both in the rim and in the pellet interior.

2.4. Temperature Distribution in a Pellet Containing Rim Region

To calculate the temperature distribution across fuel radius, a pellet is divided into several concentric

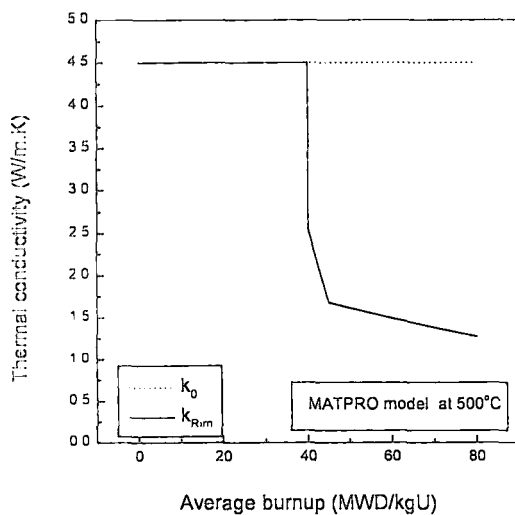


Fig. 4(a). Thermal Conductivity at Pellet Interior and Rim Region from MATPRO Model[11].

rings of equal mass. Then the steady-state thermal conduction equation is solved for each ring. Taking the temperature of the outer surface of pellet as a basis, temperatures at the boundaries of each ring are determined from the pellet outside towards the inside up to the pellet center.

If the outer temperature of the j -th ring, T_{j+1} , is

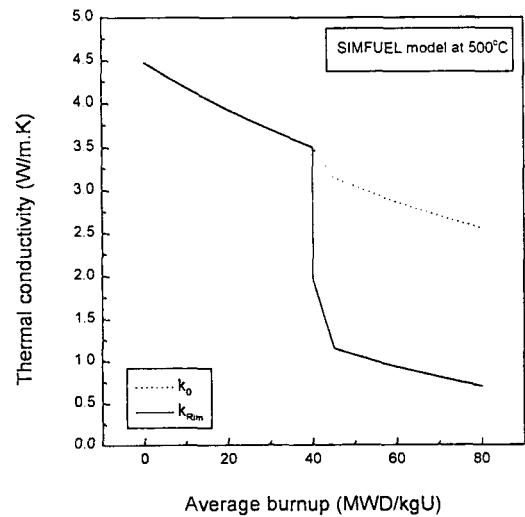


Fig. 4(b). Thermal Conductivity at Pellet Interior and Rim Region from SIMFUEL Model[10].

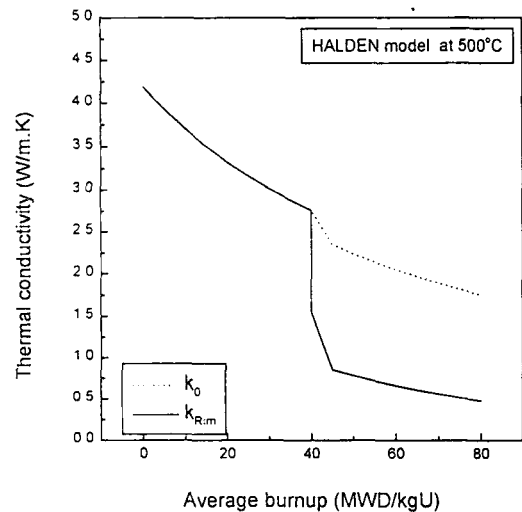


Fig. 4(c). Thermal Conductivity at Pellet Interior and Rim Region from HALDEN Model[12].

known, the inner temperature of the j -th ring, T_i , in the j -th ring is calculated from the following equation [18]:

$$\int_{T_{j+1}}^{T_j} k_j(T, BU_j) dT = \frac{1}{4\pi H_j} \cdot \left(q_j - 2 \cdot \frac{R_j^2 \cdot Q_{j+1} - R_{j+1}^2 \cdot Q_j}{R_{j+1}^2 - R_j^2} \cdot \ln \left(\frac{R_{j+1}}{R_j} \right) \right) \quad (11)$$

where

BU_j = bumup of the j -th ring

R_j = inner radius of the j -th ring

R_{j+1} = outer radius of the j -th ring

H_j = pellet height of the j -th ring

Q_j = power released in a fractional pellet volume from R_i to R_j

Q_{j+1} = power released in a fractional pellet volume from R_i to R_{j+1}

As mentioned before, since radial power density across the pellet radius is a function of burnup, initial enrichment and fuel rod geometry, radial power depression should be considered to calculate the temperature distribution. If we denote q_j as the power of the j -th ring, it is related to the average power of a pellet q_{avg} as follows:

$$q_j = g_j \cdot q_{avg} \quad (12)$$

where g_j is the power depression factor in the j -th ring. This parameter is obtained from the FACTOR [14].

To calculate the temperature in the porous rim, Eqs. (9) and (11) are combined. First "old" temperature at the inner boundary of the rim region is assumed and from this we get the average temperature of the rim region. Using the thermal conductivity obtained at this average temperature, "new" temperature at the inner boundary of the rim region is calculated. This process is repeated until the difference between the calculated (new) and assumed (old) temperature is less than 1°C. Once the inner temperature of the rim region is determined in this way, all the temper-

atures at the boundary of each ring are calculated by the same way. Finally, the centerline temperature of the pellet T_1 is obtained from

$$\int_{T_2}^{T_1} k_1(T, BU_1) dT = \frac{q_1}{4\pi H_1} \quad (13)$$

3. Results and Discussion

Using Eqs. (9) and (11), radial temperature distributions are calculated and compared with the RISO and HALDEN experimental results. Fig. 5 shows the comparison for the RISO data for the linear heat generation rates of 30, 35 and 40 kW/m at the pellet average burnup of 43.5 MWD/kgU.

The radial temperature profile calculated using the MATPRO's correlation for thermal conductivity is compared with the RISO data in Fig. 5(a). This figure shows that the calculated temperatures are much lower than the measured ones across the pellet radius. This difference can be explained from the fact that the MATPRO's correlation does not consider the effect of burnup on the degradation of thermal conductivity which would be significant at 43.5 MWD/kgU. Temperature jump in the rim region, which is expected to occur at this burnup, is not observed in this case due to the following reason. As Eq. (9) displays, thermal conductivity developed in this study is composed of two terms; one for the degradation with burnup across pellet radius and the other for the degradation due to high porosity in the rim region. Therefore, the MATPRO's thermal conductivity, which does not consider the burnup effect, is large enough to offset the conductivity decrease in the rim region due to high porosity. This leads to the absence of the temperature jump in the rim region.

Fig. 5(b) shows the comparison when the thermal conductivity correlation obtained from the SIMFUEL data is used. In contrast to Fig. 5(a), although the difference between the calculated and measured temperatures is slightly reduced, considerable discrep-

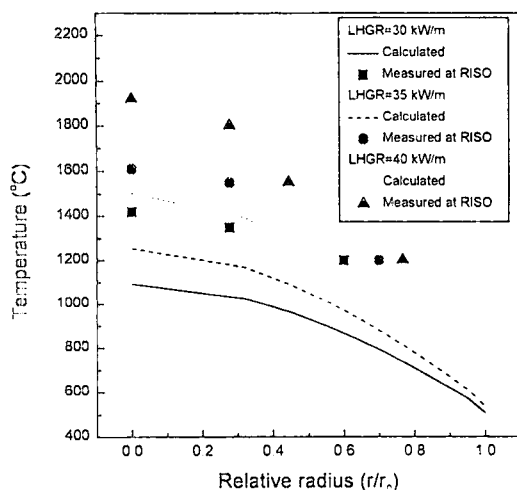


Fig. 5(a). Comparison of Calculated Radial Temperature Distribution Based on MATPRO Model with the Measured RISO Data at the Pellet Average Burnup of 43.5 MWD/kgU.

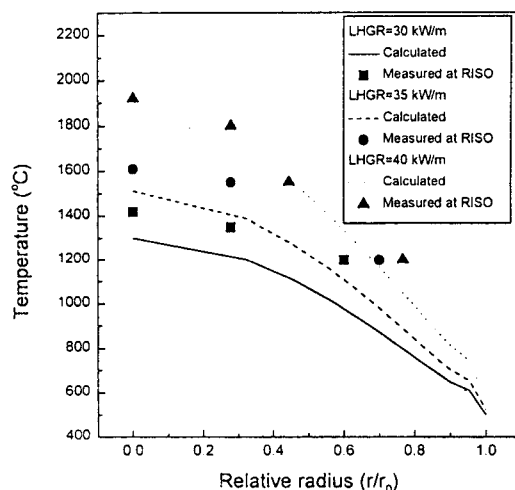


Fig. 5(c). Comparison of Calculated Radial Temperature Distribution Based on HALDEN Model with the Measured RISO Data at the Pellet Average Burnup of 43.5 MWD/kgU.

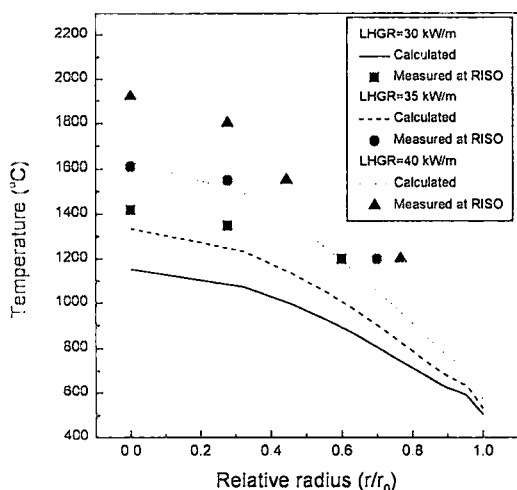


Fig. 5(b). Comparison of Calculated Radial Temperature Distribution Based on SIMFUEL Model with the Measured RISO Data at the Pellet Average Burnup of 43.5 MWD/kgU.

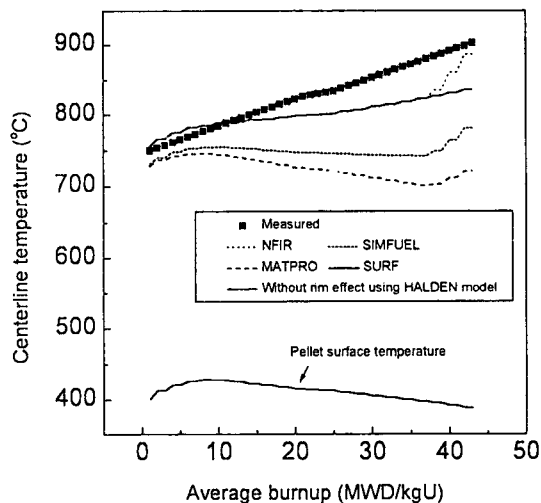


Fig. 6. Calculated and Measured Centerline Temperature of UO_2 Fuel at Linear Heat Rating of 25kW/m

ancy still exists. Of the factors that degrade the thermal conductivity of irradiated fuel, SIMFUEL has only precipitated and dissolved fission products and does not contain fission gas bubbles and volatile fission products [10]. Therefore, it is expected that the

thermal conductivity derived from the SIMFUEL data would be larger than that for the irradiated fuel since there would be no degrading effects of the fission gas bubbles and volatile fission products on the thermal conductivity, resulting in lower fuel temperature.

In addition, a slight temperature jump in the rim is observed. The temperature jump across the porous rim region is about 200°C and the surface temperature of fuel is nearly 600°C . Temperature jump at the pellet edge and the surface temperature obtained here are consistent with the RISO's experimental results [15].

On the other hand, good agreement is obtained when the HALDEN's correlation derived from irradiated fuel is applied with additional temperature jump being observed in the rim region as shown in Fig. 5(c). This indicates that the assumption that all gas atoms produced in the rim region are retained in the porosity, which was used in deriving Eq. (9), is reasonable. However, for the linear heat generation rates of 30 and 35 kW/m, the calculated temperatures are about 100°C lower than the measured ones at the central parts of pellet. At present, it is difficult to find out where these differences come from. One possible explanation is that there are many uncertainties which were not considered in the present analysis due to the lack of relevant information. Another probable cause is that the HALDEN's thermal conductivity was evaluated to be higher than the real value thus leading to lower calculated temperature. It is likely that the latter explanation is more convincing from Fig. 5(c) which shows that calculated temperatures are generally lower than measured ones.

Fig. 6 presents the comparison with HALDEN data measured at 25 kW/m as a function of burnup in a fuel rod with small diametrical gap operating at temperatures below 1000°C [16]. The calculated surface temperature of the pellet is also shown as a function of burnup. The measured centerline temperature increases continuously with burnup mainly due to degradation of thermal conductivity. Since it was assumed in Sec.2.3 that threshold pellet average burnup for the formation of rim region is 40 MWD/kgU, the temperature jump appears in the present calculation at burnups higher than 40MWD/kgU. When the HALDEN model is used, the calculated temperature without considering rim effect increases lin-

early, while the calculated temperature with rim effect considered shows steep increase after the threshold burnup. The other two correlations underpredict fuel centerline temperature by the same explanations given for Figs. 5(a) and 5(b). Although the relationship for correlating pellet average burnup with rim burnup shows very wide statistical scattering as can be seen in Fig. 1, the thermal conductivity model developed in this paper seems to well predict the temperature variations even in the burnup higher than 40 MWD/kgU.

4. Conclusions

Based on the MATPRO, SIMFUEL and HALDEN's correlation for thermal conductivity, a thermal conductivity correlation has been proposed that can be applied to both pellet interior and highly porous pellet rim. In addition, a correlation has been developed that can estimate the porosity of rim region as a function of rim burnup under the assumptions that all the fission gases produced in the rim region are retained in the rim porosity and threshold pellet average burnup required for the formation of rim region is 40 MWD/kgU. Rim width is correlated to rim burnup using measured data.

Calculated radial temperature distributions using the correlation developed in this paper were compared with the RISO experimental data obtained at the pellet average burnup of 43.5 MWD/kgU for the three linear heat generation rates of 30, 35 and 40 kW/m, respectively. Best agreement was obtained when the thermal conductivity correlation developed in this paper is combined with the HALDEN's correlation for the degrading thermal conductivity with burnup. On the other hand, both MATPRO conductivity which does not consider the effect of burnup on the degradation of thermal conductivity and SIMFUEL conductivity obtained from the absence of fission gas bubbles and volatile fission products give lower fuel temperatures. This comparison indicates that both the degradation of thermal conductivity with burnup

and the temperature jump in the rim region due to high porosity should be taken into account in analyzing high burnup fuel.

Another comparison with the HALDEN's fuel centerline temperature measured as a function of burnup at 25 kW/m suggests that best agreement is made also when the present correlation is combined with the HALDEN's thermal conductivity, although the slopes of increase in fuel centerline temperature with burnup are different for the calculated and measured temperatures.

Through these two comparisons, it is concluded that a thermal conductivity correlation proposed in this paper can be used to calculate the temperature distribution in high burnup fuel by considering both the degradation of thermal conductivity with burnup across fuel pellet and additional degradation in pellet rim due to very high porosity. Using the SIMFUEL's thermal conductivity produces lower temperature due to the characteristics of SIMFUEL, which does not consider the effects of fission gas bubbles and other volatile fission products produced during irradiation of fuel. It is not appropriate to use the MATPRO's thermal conductivity for the analysis of fuel behavior at high burnup because it does not consider the effect of burnup on the degradation of thermal conductivity degradation with burnup.

References

1. K. Lassmann, C. O'Carroll, J. van de Laar and C.T. Walker, "The radial distribution of plutonium in high burnup UO_2 fuels," *Journal of Nuclear Materials*, 208, **223** (1994)
2. J.O. Barner, M.E. Cunningham, M.D. Freshley and D.D. Lanning, "Relationship between microstructure and fission gas release in high burnup UO_2 fuel with emphasis on the rim region," *International Topical Meeting on LWR Fuel Performance*, Avignon, France, April 21-24, (1991)
3. H.J. Matzke, "On the rim effect in high burnup UO_2 LWR fuels," *Journal of Nuclear Materials*, **189**, 141 (1992)
4. M.E. Cunningham, M.D. Freshley and D.D. Lanning, "Development and characteristics of the rim region in high burnup UO_2 fuel pellets," *Journal of Nuclear Materials*, **188**, 19 (1992)
5. S.R. Pati, A.M. Gared, and L.J. Clink, "Contribution of pellet rim porosity to low-temperature fission gas release at extended burnup," *International Topical Meeting on LWR Fuel Performance*, Williamsburg, Virginia, April 17-20, (1982)
6. N. Kjaer-Pederson, "Rim effect observations from the third RISO fission gas project," *Proceedings of a technical committee meeting*, Ontario, Canada, April 28, p. 111, (1992)
7. J. O. Barner, M. E. Cunningham, M. D. Freshley and D. D. Lanning, "Evaluation of fission gas release in high-burnup LWR fuel rods," *Nuclear Technology*, **102**, 210 (1993)
8. R. Manzel and R. Eberle, "Fission gas release at high burnup and the influence of the pellet rim," *International Topical Meeting on LWR Fuel Performance*, Avignon, France, April 21-24, (1991)
9. K. Lassmann, C. T. Walker, J. van de Laar, F. Lindstrom, "Modelling the high burnup UO_2 structure in LWR fuel," *Journal of Nuclear Materials*, **226**, 1 (1995)
10. P.G. Lucuta, H.J. Hatzke, R. A. Verrall, "Modelling of UO_2 -based SIMFUEL thermal conductivity: The effect of the burnup," *Journal of Nuclear Materials*, **217**, 279 (1994)
11. MATPRO-VERSION 11 (Revision 2): A handbook of materials properties for use in the analysis for light water reactor fuel rod behavior. NUREG/CR-0497, EG&G Idaho, August, (1981)
12. Twenty Eighth NFIR Steering Committee Meeting, Halden, Norway, November, (1995)
13. H. Kampf and G. Karsten, "Effect of different types of void volumes on the radial temperature distribution of fuel pins," *Nuclear Application and Technology*, **9**, 288 (1970)

14. Y.H. Koo, "The computer program FACTOR for calculating the radial power density and burnup factors in fuel pellets," Siemens Technical Report B412/90/E84, (1990)
15. C. Bagger, M. Mogensen, and C.T. Walker, "Temperature measurements in high burnup UO₂ nuclear fuel: Implication for thermal conductivity, grain growth and gas release," *Journal of Nuclear Materials*, **211**, 11 (1994)
16. E. Kolstad and C. Vitanza, "Fuel rod and core materials investigations related to LWR extended burnup operation," *Journal of Nuclear Materials*, **188**, 104 (1992)
17. D.G. Martin, "A Reappraisal of the thermal conductivity of UO₂ and mixed (U,Pu) oxide fuel," *Journal of Nuclear Materials*, **110**, 73 (1982)
18. Dong-Seong Sohn, Fuel Rod Design Manual, Korea Atomic Energy Research Institute, (1988)